Coordination Geometry of the Copper−Pyridine Complex in Frozen Solution As Studied by Proton and Deuterium Two-Dimensional Hyperfine Sublevel Correlation Electron Spin Resonance Spectroscopy

A. Pöppl,[†] M. Hartmann,[‡] W. Böhlmann,[†] and R. Böttcher*[,†]

Fakultät für Physik und Geowissenschaften, Universität Leipzig, Linnéstr. 5, D-04103 Leipzig, Germany, and Institut für Technische Chemie I, Universität Stuttgart, D-70550 Stuttgart, Germany

Received: December 4, 1997; In Final Form: March 11, 1998

The coordination geometry of the tetrapyridine−copper(II) complex in frozen solution is investigated by proton and deuterium two-dimensional hyperfine sublevel correlation spectroscopy (HYSCORE) electron spin resonance experiments. In particular, the deuterium experiment demonstrates the potential of this method, which lies in the superior spectral resolution of the two-dimensional spectra. This allows us to resolve deuterium nuclear quadrupole splittings of the cross peak ridges even in orientationally disordered systems, which in turn yield structural information about the overall complex symmetry. Proton and deuterium experiments show pronounced cross peak ridges from protons and deuteriums at the C2 and C6 carbon atoms of the pyridine molecule. The coordination geometry within the complexes could be deduced from orientation-selective deuterium spectra. Severe deviations from the D_{4h} complex symmetry were found in such a way that the pyridine molecules are arranged with their molecular mirror plane perpendicular to the complex plane. The complex geometry experiences a significant variance with respect to the Cu−N bond directions due to random spatial constraints induced by solvent molecules.

Introduction

Electron nuclear double resonance (ENDOR) and one-dimensional (1D) electron spin-echo envelope modulation (ESEEM) spectroscopy are well-established methods for measuring weak hyperfine (hf) and nuclear quadrupole (nq) interactions in both single crystals and disordered systems. However, the interpretation of ENDOR and 1D ESEEM spectra of disordered systems is often hampered by overlapping broad signals. Two-dimensional (2D) ESEEM sequences such as the 2D four-pulse or HYSCORE (hyperfine sublevel correlation spectroscopy) experiment have been developed to solve this problem.[1] In the HYSCORE experiment ($\pi/2-\tau-\pi/2-t_1-\pi-t_2-\pi/2-\tau-$echo) the mixing π pulse creates correlations between nuclear coherences of two different electron spin (M_S) manifolds with the nuclear transition frequencies $\omega_{i,j}$ and $\omega_{l,m}$. These correlation lead to cross peaks (ω_{ij}, ω_{lm}), (ω_{lm}, ω_{ij}) or ($-\omega_{ij}$, ω_{lm}), and ($-\omega_{lm}$, ω_{ij}) in the 2D Fourier transformed (FT) spectra depending on the size of the hf and nq interaction with respect to the nuclear Larmor frequency. The spread of the spectrum into two dimensions improves significantly the spectral resolution of the FT ESEEM spectrum. Even in disordered systems, where the anisotropy of the hf and nq interactions results in a spread of the nuclear transition frequencies that leads together with the correlations between $\omega_{i,j}$ and $\omega_{l,m}$ to ridge-type cross peaks,[2,3] these cross peak ridges are well separated in many experimental cases. In such spectra the hf and nq parameters can be determined by an analysis of the position and shape of those ridges. Therefore, the 2D techniques provide essential, more spectral information, especially in disordered systems, than 1D experiments, where only broad featureless signals are observed in many spectra.

Different nuclei such as ^{1}H, ^{13}C, ^{15}N, ^{14}N, and ^{27}Al have been successfully investigated by the HYSCORE technique in orientationally disordered systems.[3−11] HYSCORE spectroscopy has been proven to be a powerful tool especially for the investigation of ^{14}N ligand nuclei in biological systems, where the nitrogen nq interaction gives rise to complicated ESEEM spectra with heavily overlapping signals.[7−10] The improved spectral resolution of the HYSCORE experiment leads to a separation of the different nitrogen hf signals that overlap in the 1D ESEEM spectra and allows an unambiguous assignment of the signals to the $\Delta M_I = \pm 1$ and $\Delta M_I = \pm 2$ nuclear transitions. On the basis of these 2D experiments, the principal values and direction cosines of the ^{14}N hf and nq interactions could be determined by orientation-selective ESEEM measurements even in powder samples.[8,9]

Surprisingly, the potential of the HYSCORE technique has not been utilized for the investigation of deuterium ligand nuclei to our knowledge up to now. We assume that the high spectral resolution of the HYSCORE experiment should allow us to measure well-resolved deuterium cross peaks, offering new possibilities for the determination of deuterium hf and nq interactions in disordered systems. In a previous paper, we have shown that only 4 out of 16 possible deuterium cross peaks from $\Delta M_I = \pm 1$ nuclear transitions will appear in the 2D spectra with sufficient intensity.[12] The reduction in the number of observable cross peaks leads to a drastic simplification and an improved spectral resolution in the 2D spectra. Furthermore, it has been shown that the special properties of the deuterium cross peak intensities allow us to separate the hf and nq interactions in the 2D powder patterns.[12] The anisotropy of the hf interaction gives rise to ridges perpendicular to the frequency diagonal $\omega_1 = \omega_2$ of the 2D spectrum, whereas the nq coupling is mapped parallel to the $\omega_1 = \omega_2$ axis. Therefore, deuterium

[†] Universität Leipzig.
[‡] Universität Stuttgart.

S1089-5639(98)00406-X CCC: $15.00
Published on Web 04/28/1998

HYSCORE experiments do not only allow a determination of the principal values of the hf interaction tensor **A** and the nq interaction tensor **Q** but also of the relative orientation of the two tensors to each other. The orientations of both tensors **A** and **Q** with respect to the electron Zeeman interaction tensor **g** can be revealed from the 2D spectra in cases where orientation-selective ESEEM experiments are possible. Especially in the investigation of transition metal ion complexes, deuterium HYSCORE experiments should give access to more detailed information about the coordination geometry and ligand arrangement than proton HYSCORE spectra. Basically, the magnitude of the isotropic and dipolar hf interaction A_{iso} and $T_\perp$ as well as the orientation of the dipolar hf interaction tensor with respect to the tensor **g** of the transition metal ion can be derived from analysis of the shape of the cross peak ridges in orientation-selective proton HYSCORE spectra.[3,4,13] However, it seems to be vague to deduce the coordination geometry from proton HYSCORE spectra alone, especially in cases where the spin density is delocalized over the metal ion complex or where a spatial disorder in the ligand arrangement is present. In such cases, the determination of the orientation of the deuterium nq interaction tensor with respect to the deuterium hf tensor and **g** coordinate system by orientation-selective HYSCORE spectra might provide a more direct access to the coordination geometry in metal ion complexes with deuterated ligands.

In this paper we present a study of the coordination geometry of the tetrapyridine−copper(II) complex in frozen solution by means of proton and deuterium HYSCORE spectroscopy. The study illustrates the potential of the deuterium HYSCORE experiment. At the beginning we briefly discuss the differences between proton and deuterium HYSCORE spectra in disordered systems. In the Experimental Section orientation-selective 2D ESEEM experiments are presented, which allow a determination of the hf tensor of the proton/deuterium at the C2 and C6 carbon atoms of the pyridine ligand. The arrangement of the ligands with respect to the Cu(II) **g** tensor frame is deduced from an analysis of the nq coupling in the deuterium 2D HYSCORE spectra. The experiments reveal a spatial disorder of the arrangement of the ligands. The results are supported by simulations of the deuterium HYSCORE powder spectra.

Deuterium versus Proton HYSCORE in Disordered Systems

The general expression for the modulation of the four-pulse ESEEM

$$E_{mod}(\tau, t_1, t_2) = \sum_{ijklmn} M_{il}M_{lj}^{+}M_{jm}M_{mk}^{+}M_{kn}M_{nl}^{+}\, e^{-i(\omega_{ij}\tau+\omega_{ik}t_2+\omega_{ln}\tau+\omega_{lm}t_1)} + \sum_{ijklmn} M_{il}M_{lj}^{+}M_{jm}M_{mk}^{+}M_{kn}M_{ni}^{+}\, e^{-i(\omega_{ik}\tau+\omega_{jk}t_1+\omega_{mn}\tau+\omega_{ln}t_2)} + c.c. \quad (1)$$

has been derived by Reijerse et al.[8] Here, ω_{ij} denotes the nuclear transition frequencies and the quantity **M** represents the ESR transition probabilities between the nuclear spin sublevels in the two different electron spin states M_S. The *i, j, k* run over the α ($M_S = {}^1/_2$) and the *l, m, n* over the β ($M_S = -{}^1/_2$) manifold.

In the case of protons ($I = {}^1/_2$), *i, j, k* = 1, 2 and *l, m, n* = 1, 2 and the two nuclear transition frequencies in the two $M_S = \pm{}^1/_2$ electron spin manifolds are commonly designated by ω_α and ω_β. The frequencies ω_α and ω_β and the matrix **M** of the ESR transition probabilities of the $S = {}^1/_2$, $I = {}^1/_2$ spin system

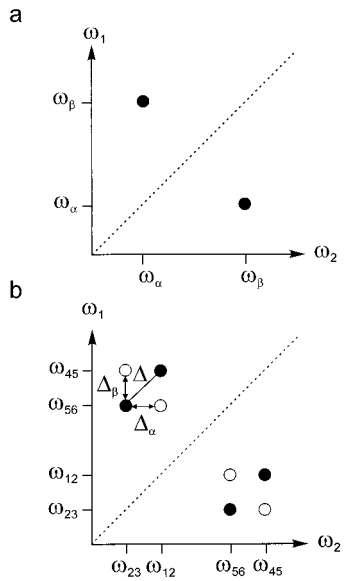

Figure 1. Schematic single-crystal HYSCORE spectrum for the case $A_{zz} < \omega_I/\pi$: (a) proton spectrum and (b) deuterium spectrum where only cross peaks from $\Delta M_I = \pm 1$ transitions are displayed. The solid circles represent cross peaks with intensities proportional to the modulation depth parameter *k*, whereas open circles indicate cross peaks proportional to k^n, $n > 1$. The dashed lines show the frequency diagonal axis $\omega_1 = \omega_2$.

can be calculated from the standard spin Hamiltonian

$$\hat{H} = \beta_e \mathbf{B}_0 \mathbf{g} \hat{\mathbf{S}} - g_n \beta_n \mathbf{B}_0 \hat{\mathbf{I}} + \hat{\mathbf{S}} \mathbf{A}^P \hat{\mathbf{I}} \quad (2)$$

where $\mathbf{A}^P$ is the proton hf coupling tensor. All other symbols have their usual meanings. The Hamiltonian in eq 2 is given in frequency units. Explicit expressions for the modulation in the 2D HYSCORE experiment of the $S = {}^1/_2$, $I = {}^1/_2$ spin system have been given by Gemperle et al.[14] The nuclear transition frequencies ω_α and ω_β are determined by the two equations[15]

$$\omega_{\alpha/\beta} = \omega(M_S) = |(\tilde{\mathbf{I}}\mathbf{C}(M_S)\tilde{\mathbf{C}}(M_S)\mathbf{l})^{1/2}| \quad (3)$$

and

$$\mathbf{C}(M_S) = M_S 2\pi \mathbf{A} - \omega_I \mathbf{E} \quad (4)$$

where **E** is the identity matrix, ω_I the nuclear Larmor frequency, and **l** denotes the unit vector along the external magnetic field.

In the case of cupric ion complexes the proton ligand hyperfine interaction is usually small, $A_{zz}^P < \omega_I/\pi$. Then the cross peaks will be situated in the upper quadrant of a single-crystal 2D FT spectrum at (ω_α, ω_β) and (ω_β, ω_α) as schematically shown in Figure 1a. In disordered systems the anisotropy of the hf interaction results in a spread of the nuclear transition frequencies, which leads together with the correlations between ω_α and ω_β to two different cross peaks ridges. These ridges are directed perpendicular to the frequency diagonal $\omega_1 = \omega_2$ in the case of small hf interaction, $A_{zz}^P < \omega_I/\pi$. This is illustrated in Figure 2a, where a simulation of a powder proton HYSCORE spectrum is presented. In the simulation an axially symmetric electron **g** tensor was assumed with a microwave irradiation at the $g_\perp$ spectral position within the ESR powder pattern. Furthermore, the *z* axis of the axially symmetric proton hf tensor $\mathbf{A}^P$ was chosen to be within the $g_\perp$ plane. The HYSCORE spectrum was computed in the time domain using the general expression of the four-pulse ESEEM experiment in eq 1. For the simulation, the angle $\theta_g = 90°$ between the $g_{||}$

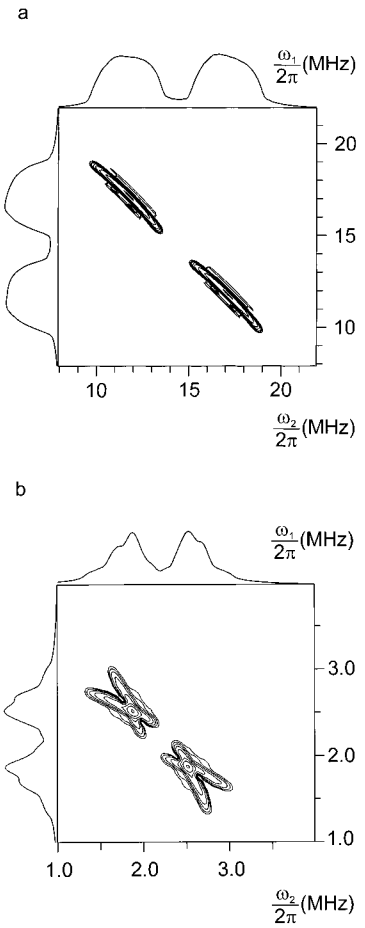

Figure 2. Simulated proton and deuterium powder HYSCORE spectra for an axially symmetric **g** tensor with $g_{\|} = 2.238$ and $g_{\perp} = 2.061$ and microwave irradiation at the $g_{\perp}$ spectral position: (a) proton spectrum with simulation parameters $\tau = 32$ ns, $\omega_I = 14.21$ MHz, $A_{xx} = A_{yy} = 1.50$ MHz, $A_{zz} = 9.30$ MHz; (b) deuterium spectrum with simulation parameters $\tau = 224$ ns, $\omega_I = 2.18$ MHz, $A_{xx} = A_{yy} = 0.22$ MHz, $A_{zz} = 1.46$ MHz, $Q_{xx} = Q_{yy} = -45$ kHz and $Q_{zz} = 90$ kHz.

axis of the axially symmetric **g** tensor and the external magnetic field is fixed and the integration is performed over the azimuthal angle ϕ

$$\langle E_{\mathrm{mod}} \rangle = (1/\pi)\int_0^{\pi} E_{\mathrm{mod}}(\theta_g = 90°, \phi)\, \mathrm{d}\phi \qquad (5)$$

The nuclear transition frequencies ω_{ij} were calculated by an exact diagonalization of the total spin Hamiltonian matrix (eq 2) of the $S = {}^1/_2$, $I = {}^1/_2$ spin system. The elements of the state-mixing matrix **M** were calculated from the matrix elements $M_{il} = \langle \Phi_i | S_x | \Phi_l \rangle$. The Φ_i and Φ_l are the eigenvectors of the spin Hamiltonian matrix, whereas the indices i and l run over the α ($M_S = -{}^1/_2$) and β ($M_S = {}^1/_2$) manifold, respectively. Finally, the time domain spectrum was zero-filled, Fourier transformed, and displayed as a magnitude spectrum.

In the case of deuterium ($I = 1$) the spin Hamiltonian has to be expanded by the nq interaction term

$$\hat{H} = \beta_e \mathbf{B}_0 \mathbf{g} \hat{\mathbf{S}} + \hat{\mathbf{S}} \mathbf{A}^{\mathrm{D}} \hat{\mathbf{I}} - g_n \beta_n \mathbf{B}_0 \hat{\mathbf{I}} + \hat{\mathbf{I}} \mathbf{Q} \hat{\mathbf{I}} \qquad (6)$$

where **Q** is the deuterium nq interaction tensor. Since we may assume for deuteriums that the nq interaction is small in comparison with the hf and nuclear Zeeman interaction, the nuclear frequencies are given by the first-order perturbation theory[15]

$$\begin{aligned} \omega_{12} &= \omega_\alpha + \Delta_\alpha \quad \omega_{45} = \omega_\beta + \Delta_\beta \\ \omega_{23} &= \omega_\alpha - \Delta_\alpha \quad \omega_{56} = \omega_\beta - \Delta_\beta \\ \omega_{13} &= 2\omega_\alpha \quad \omega_{46} = 2\omega_\beta \end{aligned} \qquad (7)$$

Here, the nq frequencies $\Delta_{\alpha/\beta}$ are calculated according to[15]

$$\Delta_{\alpha/\beta} = \Delta(M_S) = 2\pi \frac{3\tilde{\mathbf{I}}\mathbf{C}(M_S)\mathbf{Q}\tilde{\mathbf{C}}(M_S)\mathbf{l}}{2\omega_{\alpha/\beta}^{\ 2}} \qquad (8)$$

Again, the modulation expression in the deuterium 2D HYSCORE experiment can be derived from eq 1 where now $i, j, k = 1, 2, 3$ and $l, m, n = 4, 5, 6$. Basically, we would expect eight cross peaks of $\Delta M_I = \pm 1$ transitions in the upper quadrant of the deuterium FT 2D spectrum, which are situated in the upper quadrant in the limit $A_{zz}^{\mathrm{D}} < \omega_I/\pi$. However a recent analysis[12] of the cross peak intensities revealed that the peaks at (ω_{12}, ω_{56}), (ω_{23}, ω_{45}), (ω_{56}, ω_{12}), and (ω_{45}, ω_{23}) have intensities that are proportional to the power of 2 or higher in the modulation depth parameter k. As in ESEEM experiments, usually $k \ll 1$ holds so that those peaks will not appear in the 2D spectra with sufficient intensity and the spectra will only display peaks at (ω_{12}, ω_{45}), (ω_{23}, ω_{56}), (ω_{45}, ω_{12}), and (ω_{56}, ω_{23}). This special property of the cross peak intensities gives rise to a reduction in the number of observable cross peaks, which results in a drastic simplification of the spectra. The situation is illustrated in Figure 1b. If we compare the depicted deuterium HYSCORE spectrum with the proton spectrum, we see that the deuterium nq interaction leads to a splitting of the observable cross peaks parallel to the frequency diagonal $\omega_1 = \omega_2$.

It is worth mentioning that the anisotropic hf interaction spreads the cross peak ridges perpendicular to the $\omega_1 = \omega_2$ axis in disordered systems. Therefore, the nq and hf interactions are partially separated in the deuterium 2D powder spectrum and we expect a splitting of the cross peak ridges due to the nq interaction. As an example, a simulated deuterium 2D powder spectrum is illustrated in Figure 2b. The spectrum was computed in the same way as the proton spectrum in Figure 1a except the Hamiltonian in eq 5 was used. An axially symmetric **Q** tensor was assumed in the simulation, whose principal axes frame is coaxial to the deuterium hf interaction tensor $\mathbf{A}^{\mathrm{D}}$. The splitting of each cross peak ridge into two ridges due to the nq interaction is clearly visible in the deuterium 2D spectrum (Figure 2b). The crossing of the split ridges is a consequence of the traceless tensor **Q** causing a change in the sign of the nq splitting $\Delta_{\alpha/\beta}$. In general, the properties of the deuterium 2D cross peak pattern allow us to determine the orientation of the nq tensor with respect to the deuterium hf tensor from an analysis of the splitting of the ridges at various positions within the ridges. In some cases, where two principal axes of the nq tensor are within the $g_{\perp}$ plane, the principal values of the nq tensor can be deduced from a single orientation-selective 2D spectrum taken at the $g_{\perp}$ spectral position. However, the splitting Δ of the ridges measured parallel along the $\omega_1 = \omega_2$ axis can only be regarded as a rough estimate for the nq splitting, since the deuterium nq frequencies in the two M_S states might be different for various orientations within the powder pattern. This effect is caused by different orientations of the quantization axis of the nuclear spin in the two M_S manifolds due to the anisotropic hf interaction. This effect manifests itself in a tilt of the maximum nq splitting of the cross peaks away from the $\omega_1 = \omega_2$ axis. Therefore, spectral simulations of the 2D spectra

seem to be necessary to deduce the exact orientation of the tensors to each other.

Experimental Section

Copper−pyridine complexes were prepared from copper chloride and pyridine ($[Cu(NC_5H_5)_4]^{2+}$) or fully deuterated pyridine ($[Cu(NC_5D_5)_4]^{2+}$).[16] A 1 mmol solution of cupric ions in pyridine was used in both cases and was filled in quartz glass tubes. After being sealed, the tubes were rapidly frozen in liquid nitrogen. The procedure provided glassy samples of frozen solution without using glass builders such as glycerol. The formation of the tetrapyridine−copper(II) complex in frozen solution was checked by ESR spectroscopy at 77 K.

ESR spectra were recorded on an ESP 300 BRUKER spectrometer at 77 K. Two-dimensional ESEEM experiments were performed on a BRUKER ESP 380 FT-ESR spectrometer at 4.2 K using the HYSCORE sequence ($\pi/2-\tau-\pi/2-t_1-\pi-t_2-\pi/2-\tau-$echo). Orientation-selective HYSCORE spectra were measured at the $g_{||}$ spectral position of the Cu(II) ESR powder pattern at 2773 G and at the $g_\perp$ position at 3773 G. Pulse lengths of 24 ns for $\pi/2$ pulses and 48 ns for π pulses were used in proton spectra. Pulse delays of $\tau = 32$ ns or $\tau = 40$ ns were chosen in the orientation-selective 2D spectra to minimize blind spots in the HYSCORE powder pattern. The HYSCORE echo was detected via a remote echo sequence ($\pi/2-t_R-\pi/2-\tau_R-\pi-\tau_R-$echo),[3] since the dead time exceeds 32 ns in our experimental setup. The pulse delays of the remote echo sequence were $t_R = 4\ \mu$s and $\tau_R = 120$ ns. An eight-step phase cycle suggested by Gemperle et al.[14] was used to avoid interference with unwanted two- and three-pulse echoes. A 170 × 170 2D data matrix was sampled with a dwell time of 16 ns. In the deuterium spectra pulse lengths of 48 ns for $\pi/2$ pulses and 32 ns for π pulses were chosen to suppress diagonal peaks in the 2D spectra. The combination of relatively soft $\pi/2$ pulses and hard π pulses ensures an efficient exchange of the nuclear coherences between the two different M_S states by the mixing π pulse. This is a necessary condition for the observation of cross peaks in the 2D four-pulse experiment and especially critical for low-frequency nuclear transitions. Pulse delays of $\tau = 224$ ns or $\tau = 272$ ns were used to enhance deuterium modulation. Likewise, a 170 × 170 2D data matrix was sampled using the eight-step phase cycle. The dwell time was 64 ns. The echo decay was eliminated by a third-order polynomial baseline correction of the experimental data set in both time domains. Two-dimensional FT magnitude spectra were calculated and presented as contour plots.

Results

The ESR spectrum at 77 K of the copper−pyridine complex in the frozen solution is illustrated in Figure 3. The spectrum can be described by an axially symmetric Cu(II) **g** tensor with $g_{||} = 2.262$, $g_\perp = 2.055$, and a metal ion hyperfine splitting of $A_{||} = 174 \times 10^{-4}$ cm^{-1}. A close inspection of the $g_{||}$ and $g_\perp$ spectral regions of the Cu(II) powder pattern reveals a super hf splitting (shfs) into nine lines. The number of shfs lines is suggestive of four equivalent nitrogen nuclei interacting with the unpaired electron. The nitrogen super hf splitting determined from the $g_\perp$ spectral region of the Cu(II) powder pattern is $A^N = 13 \times 10^{-4}$ cm^{-1}. A slightly smaller value $A^N = 11 \times 10^{-4}$ cm^{-1} was measured at the $g_{||}$ position. The Cu(II) $g_{||}$ and $A_{||}$ parameters together with the nitrogen shfs splitting are indicative of a coordination of the cupric ion to four pyridine ligands in a square-planar coordination geometry.[16−20] Consequently, copper−pyridine complexes exist in the form of $[Cu(NC_5H_5)_4]^{2+}$ in the frozen solution. Comparable spectra were obtained for deuterated pyridine solutions.

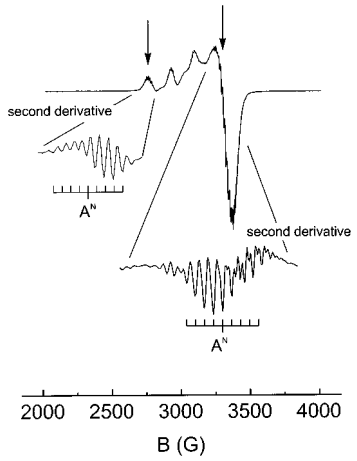

Figure 3. ESR spectrum of the copper−pyridine complex in frozen solution at 77 K. The arrows indicate the spectral positions, where orientation-selective ESEEM spectra were measured.

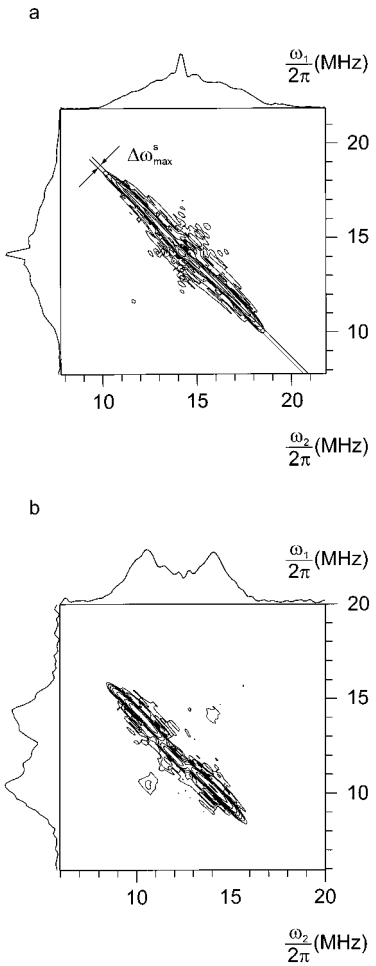

Figure 4. Experimental HYSCORE spectra of a $[Cu(NC_5H_5)_4]^{2+}$ complex in frozen solution. The spectra were recorded in the (a) $g_\perp$ and (b) $g_{||}$ spectral regions. The maximum vertical shift $\Delta\omega^S{}_{max}/(2\pi)$ of the cross peak ridges from the $\omega_1 = -\omega_2$ axis in the $g_\perp$ spectrum is illustrated by a solid line.

HYSCORE spectra of the $[Cu(NC_5H_5)_4]^{2+}$ and $[Cu(NC_5D_5)_4]^{2+}$ complexes were taken at the $g_{||}$ and $g_\perp$ spectral region of the Cu(II) ESR spectrum. Both position are indicated by arrows in Figure 3. Figure 4 illustrates the HYSCORE spectra of the $[Cu(NC_5H_5)_4]^{2+}$ complex. The spectrum recorded at the $g_\perp$

position (Figure 4a) shows two pronounced ridges that are almost directed parallel to the off-frequency diagonal axis $\omega_1 = -\omega_2$, indicating protons with substantial dipolar hyperfine coupling. The small shift of the ridges from the $\omega_1 = -\omega_2$ axis toward higher frequencies is likewise caused by the dipolar part $T_\perp$ of the proton hyperfine coupling.[3,4] The ridges are overlapped in the spectral region near the proton nuclear Larmor frequency at (14.21, 14.21) MHz by signals from weakly coupled protons.

If we assume that the protons of the pyridine molecule are lying within the $g_\perp$ plane of the Cu(II) **g** tensor on the basis of the square-planar $[Cu(NC_5H_5)_4]^{2+}$ complex geometry, the hf parameter of the protons that give rise to the pronounced ridges can be estimated according to the strategy outlined in a previous paper.[4] In this case we can determine $T_\perp = 2.6$ MHz and $A_{iso} = 4.1$ MHz from the maximum shift $\Delta\omega^S_{max}/2\pi = 0.19$ MHz of the ridges from the $\omega_1 = -\omega_2$ axis and the outer end positions of the cross peak ridges. We assign these hf parameters to the two H2 and H6 protons of the pyridine ligands with a Cu(II)−H distance of 3.1 Å.[4] The other two proton positions H3/H5 and H4 of the pyridine with Cu(II)−H distances of 5.2 and 6.0 Å presumably contribute to the peak at the proton Larmor frequency. The numbering of the protons refers to those of the corresponding carbon atom, where the proton is attached (Figure 6). For the spectrum taken at the $g_{||}$ position (Figure 4b) we would expect a single crystal-type HYSCORE spectrum, since only complexes whose $g_{||}$ principal axes point along the external magnetic field contribute to the proton 2D spectrum. Instead, we observe, besides the proton Larmor frequency peak at (11.8, 11.8) MHz of the weakly coupled protons, pronounced cross peak ridges of the more strongly coupled H2 and H6 protons, indicating a variation of about 2.9 MHz in the nuclear transition frequencies. This spread in ω_α and ω_β might suggest a variance in the orientation of the dipolar proton hf coupling tensor or in the isotropic hf interaction.

Orientation-selective deuterium HYSCORE experiments were employed to distinguish between the two sources of disorder. The spectra taken at the $g_{||}$ and $g_\perp$ position are illustrated in Figure 5. The spectrum measured at the $g_\perp$ spectral region (Figure 5a) displays the typical cross peak ridges of a HYSCORE powder spectrum but with an additional splitting of the ridges parallel to the $\omega_1 = \omega_2$ axis due to the deuterium nq interaction. Both deuterium cross peak ridges together extend over 1.43 MHz, which corresponds to the spread of about 9.3 MHz of the proton spectrum (Figure 4b) regarding the ratio between the proton and deuterium nuclear Larmor frequency of about 6.51. Therefore, it is justified to assign likewise the deuterium ridges to the D2 and D6 deuteriums of the pyridine ligands. More detailed information about the orientation of the pyridine molecule with respect to the Cu(II) **g** tensor frame can be gained from the spectrum observed at the $g_{||}$ position (Figure 5b). As in the proton case, no single-crystal-type ESEEM spectrum has been observed. Two sets of cross peak ridges were resolved, which show pronounced nq splittings. The ridges near the deuterium Larmor frequency at (1.80, 1.90) and (1.90, 1.80) MHz are attributed to weakly coupled deuteriums, whereas the intense ridges at about (1.40, 2.15), (1.60, 2.30), (2.15, 1,40), and (2.30, 1.60) MHz are attributed to the strongly coupled D2 and D6 deuteriums of the pyridine ligands. The latter deuteriums show a remarkable variation in the nq splitting, which ranges from $\Delta_{max}/(2\pi\sqrt{2}) = 0.24$ MHz at the inner end positions of the ridges to approximately $\Delta_{min}/(2\pi\sqrt{2}) = 0.04$ MHz at the outer end positions. The spread in the deuterium nq splitting indicates a variance in the orientation of the Q_{zz} axis of the deuterium nq tensor with respect to the z axis of the Cu(II) **g** tensor frame.

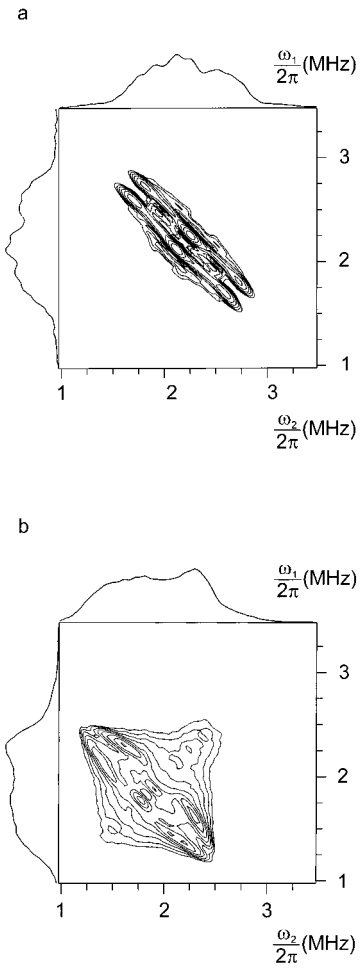

Figure 5. Experimental HYSCORE spectra of a $[Cu(NC_5D_5)_4]^{2+}$ complex in frozen solution. The spectra were recorded in the (a) $g_\perp$ and (b) $g_{||}$ spectral regions.

Discussion

The HYSCORE spectra of both protons and deuteriums, which were recorded in the $g_{||}$ spectral region of the Cu(II) ESR powder pattern, show clearly that the coordination geometry of the tetrapyridine−copper(II) complex in frozen solution is not uniform. Broad cross peak ridges have been observed instead of single crystal-type spectra in both cases. Especially the observed pronounced nq splitting of the deuterium cross peak ridges indicates a variance in the arrangement of the pyridine ligands. If we neglect possible differences in the orientation of the quantization axis of the nucleus spin in the two M_S manifolds in a first approximation, we can consider the nq splitting $\Delta/\sqrt{2}$ of the cross peak ridges in the 2D spectra as a direct measure of the nq frequency ν_Q, where

$$\frac{\Delta}{2\pi\sqrt{2}} \approx \nu_Q = \frac{3Q_{zz}}{2}(3\cos^2\theta - 1) \qquad (9)$$

holds for axially symmetric nq tensors. The quantity θ describes the angle between the z axis of the deuterium nq tensor and the external magnetic field. We have to note that the observed nq splitting in the range from $\Delta_{min}/(2\pi\sqrt{2}) = 0.05$ MHz up to $\Delta_{max}/(2\pi\sqrt{2}) = 0.24$ MHz corresponds to that of the deuterium nq coupling in the pyridine molecule ($\nu_Q(\theta = 0) = 0.27$ MHz). The principal values of the deuterium nq tensor in pyridine are

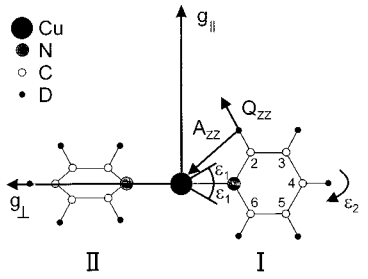

Figure 6. Schematic drawing of the $[Cu(NC_5D_5)_4]^{2+}$ complex. Only two pyridine ligands are shown for simplification. The numbers designate the different positions of carbon and proton/deuterium atoms in the pyridine ligand.

$|Q_{zz}| = 0.090$ MHz and $|Q_{xx}| = |Q_{yy}| = 0.045$ MHz where the *z* axis of **Q** points along the D2−C2 bond.[21] If we assume that the deuterium nq tensor in the pyridine ligand is only determined by the D2−C2 bond direction of the pyridine molecule, the orientation of the ligands with respect to the Cu(II) **g** tensor frame can be deduced from the 2D deuterium ESEEM spectra. The above assumption seems to be justified, since the maximum contribution of the 2-fold positive charge at the cupric ion to the **Q** tensor of the D2 deuterium is estimated to be less than 8 kHz on the basis of a simple point charge model. The same arguments hold for the symmetric D6 deuterium position.

A schematic drawing of the $[Cu(NC_5D_5)_4]^{2+}$ complex is depicted in Figure 6. Only two pyridine ligands are shown for clarification. The $g_\perp$ and $g_\parallel$ axis of the Cu(II) **g** tensor frame are parallel and perpendicular to the complex plane, respectively, which is defined by the Cu−N bonds. The pyridine ligands might have two types of disorder. One is described by a tilt of the Cu−N bond out of the complex plane (ϵ_1) and the other by a rotation around the Cu−N bond (ϵ_2). The maximum nq splitting of the cross peak ridges in the spectrum taken at the $g_\parallel$ position (Figure 4b) of $\nu_Q \approx 0.24$ MHz indicates that some of the pyridine ligand molecules have orientations with respect to the Cu(II) **g** tensor where the *z* axis of the D2 deuterium nq tensor is close to the $g_\parallel$ axis. We estimate $\theta = 12°$ for those ligands from eq 9. Of course, pyridine ligand molecules, which are with their molecular mirror plane within the $g_\perp$ plane (molecule **II** in Figure 6), have to be ruled out, since we would expect $\nu_Q(\theta = 90°) = 0.135$ MHz for them. Moreover, the magnetic field is parallel to one of the principal axes of the deuterium hf tensor of those molecules. This leads to a strong decrease in the ESEEM signal intensity as the modulation intensity drops to zero near the canonical orientations of the hf tensor. This suggests that the pyridine molecules that give rise to the pronounced cross peak ridges in the spectrum in Figure 5b are rotated by $\epsilon_2 = 90°$ around the Cu−N bond out of the complex plane. These ligands would provide an angle $\theta = 30°$ based on the geometry of the pyridine molecule. The estimated angle $\theta = 12°$ indicates a further tilt of the ligand by about $\epsilon_1 = 18°$ out of the complex plane. The *z* axis of the nq tensor of the symmetric D6 deuterium of this ligand would then form an angle of about $\theta = 48°$ with the $g_\parallel$ axis. This translates into a nq frequency $\nu_Q(\theta = 48°) = 0.045$ MHz, which is comparable to the observed splitting of the cross peak ridges at their outer end positions (Figure 5b). Therefore, we may assume that we have a variance in tilt angles in the range $0 \le |\epsilon_1| \le 18°$. It is obvious from the symmetry of the pyridine that we cannot determine the sign of the tilt angle ϵ_1 from our experiments. But it seems natural to assume a symmetric distribution of tilt angles within the limits $\epsilon_1 = \pm 18°$.

Simulations of the deuterium HYSCORE spectra have been performed to support the interpretation. The spectra were simulated according to the procedure outlined above. In the simulations a deuterium hf tensor $A_{zz} = 1.43$ MHz, $A_{xx} = A_{yy} = 0.23$ MHz determined from the proton data of the $[Cu(NC_5H_5)_4]^{2+}$ complex and a deuterium nq tensor $|Q_{zz}| = 0.090$ MHz, $|Q_{xx}| = |Q_{yy}| = 0.045$ MHz[21] was used. In general, the integration in the calculation of the orientation-selective ESEEM spectra in the case of axially symmetric **g** tensors has to be performed over the azimuthal angle ϕ and the angles ϵ_1 and ϵ_2, which describe the disorder in the ligand arrangement

$$\langle E_{mod}\rangle = \frac{1}{4\pi\Delta\epsilon_1\Delta\epsilon_2}\int_{-\Delta\epsilon_2}^{\Delta\epsilon_2}\int_{-\Delta\epsilon_1}^{\Delta\epsilon_1}\int_0^{\pi} E_{mod}(\theta_g, \phi, \epsilon_1, \epsilon_2) \times F(\epsilon_1, \Delta_1)F(\epsilon_2,\Delta_2)\, d\phi\, d\epsilon_1\, d\epsilon_2 \quad (10)$$

$F(\epsilon_1, \Delta_1)$ and $F(\epsilon_2, \Delta_2)$ with the distribution width parameters Δ_1 and Δ_2 are weighting functions for the variance in ϵ_1 and ϵ_2. The angle θ_g, which describes the orientation selection, is fixed in the calculations. For simulations of spectra at the single crystal-like $g_\parallel$ position ($\theta_g = 0$), the integration in eq 10 only has to be carried out over ϵ_1 and ϵ_2. In the simulation of the deuterium cross peak ridges in the $g_\parallel$ spectrum $\epsilon_1 = 0$, $\epsilon_2 = 90°$, and $\Delta\epsilon_2 = 0$ were set. The variance in ϵ_1 was adjusted to $\Delta\epsilon_1 = 25°$, where a Gaussian weighting function $F(\epsilon_1, \Delta_1)$ with $\Delta_1 = 30°$ was used. This parameter set corresponds to a pyridine ligand with its molecular mirror plane perpendicular to the $g_\perp$ plane and a variation in the Cu−N bond direction of $\Delta\epsilon_1 = \pm 25°$ (molecule **I** in Figure 6). The simulated spectrum is illustrated in Figure 7a, and the cross peak ridges are in good accordance with the experimental ones in Figure 5b. For comparison a simulated spectrum of a pyridine ligand with its molecular mirror plane within the $g_\perp$ plane ($\epsilon_1 = 0$, $\epsilon_2 = 0$) (molecule **II** in Figure 6) and a small disorder ($\Delta\epsilon_1 = 20°$, $\Delta\epsilon_2 = 20°$) is shown in Figure 7b. It is obvious that such an orientation of the ligands cannot account for the observed deuterium ridges. Cross peaks from those ligands are not resolved in the experimental spectrum at the $g_\parallel$ position, since this spectral region is heavily overlapped from signals of more weakly coupled deuteriums in ligand molecules such as D3, D4, and D5 and of solvent molecules.

The simulation of 2D spectra taken at the $g_\perp$ position is more complex. Beside the complexes with orientations with respect to the magnetic field described by $\theta_g = 90°$, signals of the $M_I = {}^3/_2$ Cu(II) hf transition of complexes having orientations $\theta_g = 35°$ and $\theta_g = 70°$ contribute also to the ESR spectrum at the $g_\perp$ position. This is a consequence of the anisotropy of the Cu(II) ESR spectrum, which also gives rise to the well-known extra absorption line.[22] Therefore, simulations for the three different angles θ_g have to be performed according to eq 10 and subsequently added with proper weighting factors. The weighting factors are determined by the powder line shape of the axially symmetric Cu(II) ESR spectrum. We have to note that the orientations, which contribute to the $g_\perp$ position, depend to some degree on the magnitude of the Cu(II) hf splitting in the $g_\perp$ plane. Unfortunately, the corresponding Cu(II) $A_\perp$ parameter cannot be deduced from the ESR spectrum in Figure 3. Therefore, some uncertainty in the contributing orientations θ_g remains in the simulations of the $g_\perp$ spectra. Parts a and b of Figure 8 illustrate simulated spectra where the molecular mirror plane of the pyridine ligand is perpendicular (molecule **I**) or parallel (molecule **II**) to the $g_\perp$ plane. The corresponding structural variances are $\Delta\epsilon_1 = 25°$, $\Delta\epsilon_2 = 0$ (molecule **I**) and $\Delta\epsilon_1 = \Delta\epsilon_2 = 20°$ (molecule **II**). The other simulation parameters are the same as in the spectra calculated for the $g_\parallel$ position. The simulated spectrum of molecule **I** (Figure 8a)

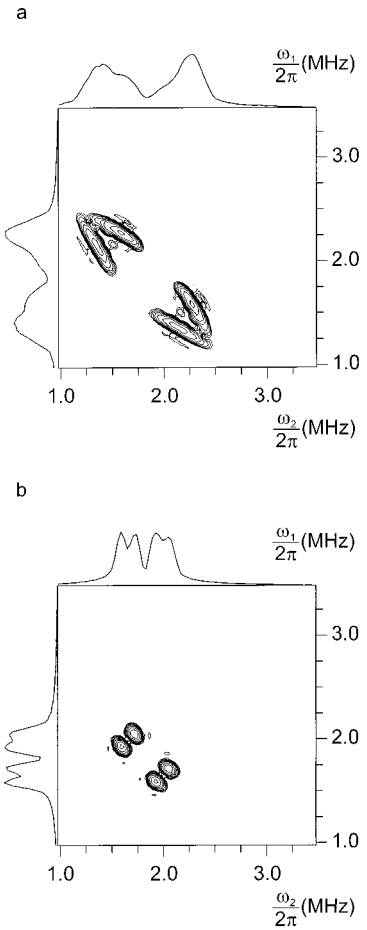

Figure 7. Simulated deuterium HYSCORE spectra for an axially symmetric **g** tensor and microwave irradiation at $g_{\|}$ ($\theta_g = 0$): (a) molecule **I** with $\epsilon_1 = 0$, $\Delta\epsilon_1 = 25°$, $\epsilon_2 = 90°$, $\Delta\epsilon_2 = 0$; (b) molecule **II** with $\epsilon_1 = 0$, $\Delta\epsilon_1 = 20°$, $\epsilon_2 = 0°$, $\Delta\epsilon_2 = 20°$. Other simulation parameters are given in the text. The cross peak intensities in (a) is 5 times of that in (b).

shows the main features of the experimental deuterium cross peak pattern in Figure 4a. Especially the outer spectral regions with their well-resolved cross peak splitting are fairly represented by the simulation. However, some details of the cross peak pattern will only be reproduced if the simulated spectrum of molecule **II** (Figure 8b) is taken into account. Especially the peaks at (1.90, 2.30), (2.20, 2.45), (2.30, 1.90), and (2.45, 2.20) MHz account for ligand arrangements such as molecule **II**. The summation of both spectra from molecules **I** and **II** provides then the best accordance with the experimental cross peak pattern. The corresponding spectrum is displayed in Figure 8c.

Analysis of the 2D spectra shows that the overall complex geometry of the tetrapyridine−copper(II) complexes in frozen solution deviates strongly from the square-planar symmetry. Deviations from the D_{4h} complex symmetry were likewise found even for $[Cu(NC_5H_5)_4]^{2+}$ complexes incorporated into single-crystal matrixes.[23] It is also obvious from steric arguments that the pyridine ligands cannot be coplanar with the $Cu-N_4$ complex plane. On the basis of our results, a part of the pyridine ligands are orientated in such a way that their molecular mirror plane is perpendicular to the complex plane to minimize spatial constraints between the ligand molecules. The complexes also show high structural flexibility, which is indicated by the variation in the Cu−N bond directions with respect to the mean complex plane. Tilts of the Cu−N bond directions up to about 25° out of the mean complex plane have been found for ligands

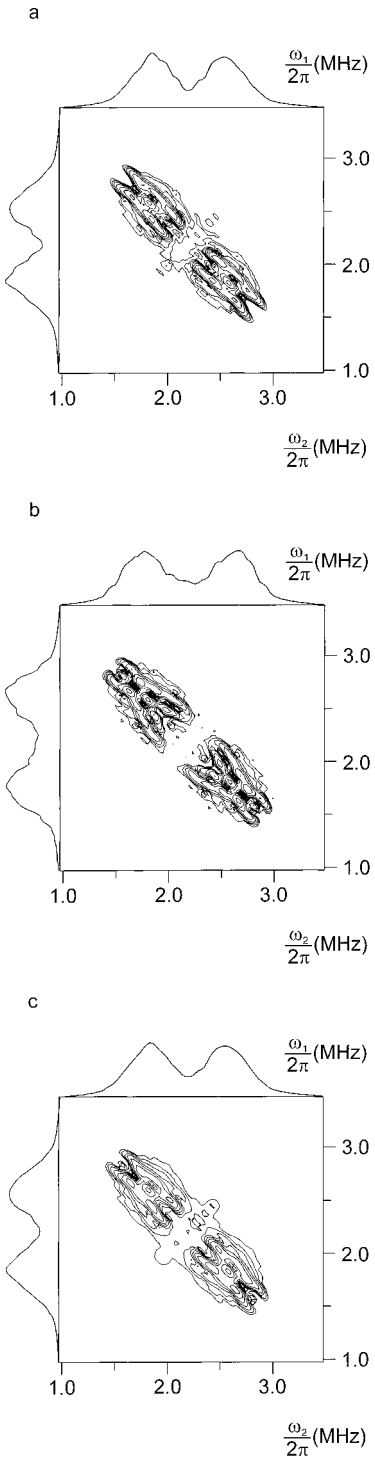

Figure 8. Simulated deuterium HYSCORE spectra for an axially symmetric **g** tensor and microwave irradiation at $g_{\perp}$ ($\theta_g = 0$): (a) molecule **I** with $\epsilon_1 = 0$, $\Delta\epsilon_1 = 25°$, $\epsilon_2 = 90°$, $\Delta\epsilon_2 = 0$; (b) molecule **II** with $\epsilon_1 = 0$, $\Delta\epsilon_1 = 20°$, $\epsilon_2 = 0°$, $\Delta\epsilon_2 = 20°$; (c) sum of the spectra in (a) and (b). Other simulation parameters are given in the text.

that have their molecular mirror plane perpendicular to the mean complex plane. This deviation from a uniform coordination geometry might be induced by spatial forces of the randomly arranged solvent molecules in the frozen solution.

It is noteworthy that our analysis of the coordination geometry relies on the unique spectral resolution of the orientation-selective deuterium 2D HYSCORE experiments. The resolved nq splitting of the cross peak ridges is a necessary condition for the investigation of deuterated complexes with some degree of structural disorder. Only additional information about the

orientation of the deuterium nq tensor with respect to the hf and **g** tensor frame allows us to distinguish between a real structural disorder and a distribution of the anisotropic hf interaction due to variations in the spin density distribution within the complexes. These results cannot be unambiguously deduced from proton HYSCORE spectra alone, where the hf coupling is the only relevant interaction.

Conclusions

In this work, we demonstrated that the HYSCORE sequence can provide highly resolved deuterium cross peak patterns in the 2D FT spectra, which allows the determination of both deuterium hf and nq coupling in orientationally disordered systems. We have to stress that the spectral resolution in the 2D spectra is superior over 1D ESEEM or ENDOR methods, where deuterium nq couplings are rarely resolved in powder spectra. However, the deuterium nq coupling yields important structural information about the overall coordination geometry in metal ion complexes with deuterated ligands. This is especially true in cases where a structural disorder in the ligand arrangement is present. Orientation-selective deuterium HYSCORE experiments give access to such information even in orientationally disordered systems. The particular application presented in this paper showed that the overall complex symmetry of the tetrapyridine−copper(II) complexes in frozen solution deviates strongly from the square-planar D_{4h} symmetry. The variation in the Cu−N bond directions presumably induced by spatial constraints of the solvent molecules indicates high structural flexibility of the tetrapyridine−copper(II) complex.

Acknowledgment. This research was supported by Deutsche Forschungsgemeinschaft, SFB 294.

References and Notes

(1) Höfer, P.; Grupp, A.; Nebenführ, H.; Mehring, M. *Chem. Phys. Lett.* **1986,** *132,* 279.
(2) Shane, J. J.; Höfer, P.; Reijerse, E. J.; De Boer, E. *J. Magn. Reson.* **1992,** *99,* 596.
(3) Höfer, P. *J. Magn. Reson., Ser. A* **1994,** *111,* 77.
(4) Pöppl, A.; Kevan, L. *J. Phys. Chem.* **1996**, *100,* 3387.
(5) Käss, H.; Rautter, J.; Bönigk, B.; Höfer, P.; Lubitz, W. *J. Phys. Chem.* **1995**, *99,* 436.
(6) Dikanov, S. A.; Samoilova, R. I.; Smieja, J. A.; Bowman, M. K. *J. Am. Chem. Soc.* **1995,** *117,* 10579.
(7) Shane, J. J.; Höfer, P.; Reijerse, E. J.; De Boer, E. *J. Magn. Reson.* **1992,** *99,* 596.
(8) Reijerse, E. J.; Shane, J. J.; De Boer, E.; Höfer, P.; Collison, D. In *Electron Paramagnetic Resonance of Disordered Systems*; Yordanov, N. D., Ed.; World Scientific: Singapore, 1991; pp 253−271.
(9) Kofman, V.; Shane, J. J.; Dikanov, S. A.; Bowman, M. K.; Libman, J.; Shanzer, A.; Goldfarb, D. *J. Am. Chem. Soc.* **1995,** *117,* 12771.
(10) Kofman, V.; Farver, O.; Pecht, I.; Goldfarb, D. *J. Am. Chem. Soc.* **1996,** *118,* 1201.
(11) Samoilova, R. I.; Dikanov, S. A.; Fionov, A. V.; Tyryshkin, A. M.; Lunina, E. V.; Bowman, M. K. *J. Phys. Chem.* **1996,** *100,* 17621.
(12) Pöppl, A.; Böttcher, R. *Chem. Phys.* **1997,** *221,* 53.
(13) Dikanov, S. A.; Bowman, M. K. *J. Magn. Reson., Ser. A* **1995,** *116,* 125.
(14) Gemperle, C.; Aebli, G.; Schweiger, A.; Ernst, R. R. *J. Magn. Reson.* **1990,** *88,* 241.
(15) Schweiger, A. *Structure and Bonding*; Springer: Berlin, 1982; Vol. 51.
(16) Ottavani, M. F. *Colloids Surf.* **1984,** *12,* 305.
(17) Turkevich, J.; Ono, Y.; Soria, J. *J. Catal.* **1972,** *25,* 44.
(18) Derouane, E. G.; Braham, J. N.; Hubin, R. *Chem. Phys. Lett.* **1974,** *25,* 243.
(19) Dai, P. S. E.; Lunsford, J. H. *Inorg. Chem.* **1980,** *19,* 262.
(20) Pöppl, A.; Kevan, L. *Langmuir* **1995,** *11,* 4486.
(21) Harris, R. K.; Mann, B. E. *NMR on the periodic table*; Academic Press: London, 1978.
(22) Ovchinnikov, I. V.; Kostantinov, V. N. *J. Magn. Reson.* **1978,** *32,* 179.
(23) Schneider, W.; v. Zelewsky, A. *Helv. Chim. Acta* **1965,** *48,* 1529.